Dielectric echo experiments on $(KBr)_{1-x}(KCN)_x$

C. Enss, H. Schwoerer,* D. Arndt,† and M. v. Schickfus
Institut für Angewandte Physik, Universität Heidelberg, Albert-Ueberle-Strasse 3-5, 69120 Heidelberg, Germany
(Received 1 July 1994)

The coherent dynamics of atomic tunneling states in $(KBr)_{1-x}(KCN)_x$ crystals in the concentration range $0.001 \geq x \geq 0.18$ have been investigated at low temperatures with two types of dielectric echo experiments at 800 MHz. In rotary echoes we find a distribution of the Rabi frequency which is very narrow in comparison with corresponding results from structural glasses. This shows that the distribution of tunnel splittings in $(KBr)_{1-x}(KCN)_x$ differs significantly from that in amorphous materials. At least from this point of view, it is doubtful whether $(KBr)_{1-x}(KCN)_x$ can be considered a model system for the low-temperature properties of the tunneling states in glasses. In addition we have investigated the temperature dependence of the phase memory and of the energy relaxation time of the tunneling states by studying the decay of the spontaneous and the stimulated echo in two- and three-pulse echo experiments.

I. INTRODUCTION

$(KBr)_{1-x}(KCN)_x$ is a dielectric mixed crystal with a sodium chloride structure in which cigar shaped CN^- molecules are randomly situated on bromium sites. Due to the similar mean radius of Br^- and CN^-, it is possible to grow single $(KBr)_{1-x}(KCN)_x$ crystals in the full CN^- concentration range x. Via their elastic quadrupole and their electric dipole-moments the CN^- molecules interact mutually and with external fields.

At room temperature the CN^- molecules rotate freely on their lattice sites. At low temperature, however, this motion freezes, the orientation of the molecules being determined by the crystal field and the elastic and electric interaction among each other.[1,2] Depending on the CN^- concentration, various ordered and disordered phases exist.[2] In the case of very low CN^- concentration ($x \lesssim 10^{-4}$) the intermolecular interaction is negligible and the isolated CN^- molecules are oriented in one of the eight $\langle 111 \rangle$ directions of the cubic KBr host crystal.[3] The potential barrier between two neighboring $\langle 111 \rangle$ orientations has been measured as $V/k_B = 35$ K.[3] Therefore, a change of orientation of the CN^- molecules at temperatures well below 35 K is only possible by quantum-mechanical tunneling through this barrier. Rotational tunneling between the eight energetically equivalent orientations results in four equidistant levels, the middle two of which being triply degenerate. A tunnel splitting splitting Δ_0/k_B between 0.6 and 1.5 K was derived from specific-heat measurements,[4,5] thermal conductivity,[6] and infrared absorption.[3,7]

With increasing concentration of CN^- ions, their individual potential becomes more and more distorted by those on nearby sites. Because of the random distribution of CN^- sites and of the strong intermolecular interaction, for $0.05 < x < 0.55$, the CN^- molecules freeze in a phase with almost random orientation,[2,8,9] called the orientational glass state. At CN^- concentrations greater than 55%, the CN^- molecules form phases with long-range orientational order.[2]

The properties of $(KBr)_{1-x}$ $(KCN)_x$ in the orientational glass state have been investigated intensively over the last decade and a detailed review of the results has been given by Höchli, Knorr, and Loidl.[10] Since measurements of the low-temperature thermal properties of $(KBr)_{1-x}(KCN)_x$ samples within this concentration range[4,5] have shown a behavior known from structural glasses, $(KBr)_{1-x}(KCN)_x$ has been suggested as a model system for an understanding of the origin of the universal low-temperature anomalies of amorphous materials.[11,12] By varying the concentration of the CN^- molecules in KBr crystals from the very dilute case to highly concentrated samples it should be possible to investigate the role of intermolecular interaction in the transition from a typical crystalline to a glasslike phase.

The results of various low-temperature experiments[13–15] have confirmed the similarity between $(KBr)_{1-x}(KCN)_x$ in the orientational glass state and structural glasses. In fact, many of these results could be described successfully using the tunneling model,[16,17] which was originally developed for glasses. Even so, it is still unclear whether $(KBr)_{1-x}(KCN)_x$ will turn out to be a useful model system to answer two long-standing questions: What is the microscopic origin of the tunneling states in amorphous materials and how can the distribution of their parameters be explained?

In connection with these questions, it will be very useful to study the dynamics of the tunneling states of this system in detail for two reasons: First, the knowledge of such detailed properties will allow a deeper understanding of the similarity of orientational and structural glasses, regarding their low-temperature properties. Second, in a model system as well defined as this, it should be possible to theoretically predict the results from a microscopic point of view.

While the coherent dynamics of tunneling states in glasses have been widely investigated,[18] only very few such experiments on $(KBr)_{1-x}(KCN)_x$ have been report-

ed so far.[19,20] To study the dynamical properties of the tunneling states in $(KBr)_{1-x}(KCN)_x$ we have performed dielectric echo experiments on samples with CN^- concentrations between $x=0.001$ and $x=0.18$ at 800 MHz and at temperatures below 100 mK. Dielectric echo experiments are a powerful tool to measure the relaxation times, the coupling constant, and the distribution of the parameters of the tunneling states.

II. THEORETICAL BACKGROUND

In this section, we will briefly review some theoretical aspects needed to describe and discuss the coherent dynamics of atomic tunneling systems. Since the key issue of this work is to compare the results of echo experiments on $(KBr)_{1-x}(KCN)_x$ with those obtained in analogous measurements on glasses, we will also discuss predictions pertaining to amorphous solids.

Instead of using the eight eigenstates expected for $\langle 111 \rangle$ tunneling of the CN^- molecules, we will simplify the problem by discussing a two-level system instead. This approach is justified because the states relevant in our resonant experiments have energy splittings on the order of 35 mK and, therefore, cannot be the unperturbed CN^- tunneling systems with a tunneling splitting of about 1 K known from the dilute case. They must originate from CN^- states whose energy spectrum is strongly modified by the interaction with strain or electrical fields from neighboring defects. Such effects have been discussed in Refs. 21 and 5 and it has been shown in Ref. 21 that interaction will lead to two lowest, closely spaced levels that are well separated in energy from the higher levels.

In the simplest case the tunneling states are described as particles with mass m moving in a double well composed of two harmonic potentials with ground-state energy E_0. The double-well potential is characterized by the barrier height V and the distance d of the wells in configurational space. Due to variations of the environment, the minima of the wells may differ by an asymmetry energy Δ. The overlap of the ground-state wave functions of the single wells leads to a tunnel splitting Δ_0. Using the WKB method Δ_0 can be estimated as

$$\Delta_0 \simeq \frac{2E_0}{\pi} e^{-\lambda}$$

with

$$\lambda \simeq \frac{d}{2\hbar}\sqrt{2mV} \ . \tag{1}$$

The total-energy splitting between the two states is given by

$$E=\sqrt{\Delta_0^2+\Delta^2} \ . \tag{2}$$

The tunneling states interact with external electrical fields $\mathbf{F}$ via their permanent electrical-dipole moment $\mathbf{p}$. Using the rotating wave approximation[22] we will assume a circularly polarized field $\mathbf{F}(t)=(F_0/2)(\hat{\mathbf{x}}\sin\omega t+\hat{\mathbf{y}}\cos\omega t)$ for the further discussion. The Hamiltonian for this problem is given by

$$H=\frac{1}{2}\begin{bmatrix} E & 0 \\ 0 & -E \end{bmatrix}+\frac{1}{E}\begin{bmatrix} \Delta & -\Delta_0 \\ -\Delta_0 & -\Delta \end{bmatrix}\mathbf{p}\cdot\mathbf{F}(t) \ . \tag{3}$$

Because we are interested in the resonant interaction with the tunneling states, the modulation of the energy splitting E by the diagonal elements in the perturbation term in Eq. (3) will be neglected henceforth. In a first-order approximation the wave function will be a linear combination of the eigenfunctions Ψ_+ and Ψ_- of the undisturbed tunneling system: $\Psi(t)=a(t)\Psi_+ + b(t)\Psi_-$. Instead of finding solutions for $a(t)$ and $b(t)$, the differential equation for the vector

$$\mathbf{S}(t)=:\begin{bmatrix} ab^*+ba^* \\ i(ab^*-ba^*) \\ aa^*-bb^* \end{bmatrix} \tag{4}$$

is set up.[23] In contrast to the formally corresponding problem of a spin $\frac{1}{2}$ in a magnetic field, the $\mathbf{S}$ space is not identical with the physical space. However, with $\mu=(\Delta_0/E)|\mathbf{p}|$ and N the number of resonant tunneling states, the physical meaning of the individual components of $\mathbf{S}$ can be interpreted as follows: $N\mu S_x=P_x$ and $N\mu S_y=P_y$ are the induced polarizations in x,y direction. $S_z=\delta N$ represents the occupation difference between the ground state and the excited state. Using this formalism the Schrödinger equation transforms into

$$\frac{\partial \mathbf{S}(t)}{\partial t}=\mathbf{h}(t)\times\mathbf{S}(t) \ ,$$

with

$$\mathbf{h}(t)=\frac{1}{\hbar}\begin{bmatrix} -\mu F_x(t) \\ -\mu F_y(t) \\ \hbar\omega \end{bmatrix} \ . \tag{5}$$

In case of resonance $\omega=E/\hbar=\omega_r$ the solution of $\mathbf{S}(t)$ is

$$S_x(t)=-\sin(\Omega_R t)\sin(\omega_r t) \ , \tag{6}$$

$$S_y(t)=\sin(\Omega_R t)\cos(\omega_r t) \ , \tag{7}$$

$$S_z(t)=-\cos(\Omega_R t) \ , \tag{8}$$

where Ω_R is the Rabi frequency, given by

$$\Omega_R=\frac{1}{\hbar}\frac{\Delta_0}{E}\mathbf{p}\cdot\mathbf{F}_0 \ . \tag{9}$$

The solution can be interpreted as the superposition of two independent motions of $\mathbf{S}$: A precession around the z axis at the resonance frequency ω_r and a nutational motion at the Rabi frequency Ω_R. For an ensemble of identical tunneling states the application of a circularly polarized rf field leads to a periodical change of the occupation number of the two levels and to a harmonical oscillation of the macroscopic polarization of the sample with Ω_R. For real systems, however, the amplitude of this oscillation decreases in time for two reasons. First, any distribution in E or Ω_R will lead to an increasingly destructive superposition of both precession and nuta-

tion. Second, the macroscopic polarization is attenuated by irreversible processes such as spontaneous emission and absorption, spin diffusion, and spectral diffusion.[24-26] These processes are taken into account phenomenologically in the Bloch equations,[27] where two relaxation times τ_1 and τ_2 are introduced. This set of equations was originally derived for spin $\frac{1}{2}$ systems in a magnetic field. Transformed into a coordinate system rotating at ω, for the case of tunneling states, the Bloch equations can be written as

$$\frac{dS_x}{dt}=-\frac{1}{\tau_2}S_x-(\omega-\omega_t)S_y\ , \tag{10}$$

$$\frac{dS_y}{dt}=(\omega-\omega_r)S_x-\frac{1}{\tau_2}S_y-\Omega_R S_z\ , \tag{11}$$

$$\frac{dS_x}{dt}=\Omega_R S_y-\frac{1}{\tau_1}(S_z-S_z^{\rm th})\ , \tag{12}$$

where $S_x^{\rm th}=-\frac{1}{2}\tanh(E/2k_BT)$ represents the thermal equilibrium value of the population difference. The longitudinal relaxation time τ_1 describes the return to thermal equilibrium after a change of the population difference. For temperatures well below 1 K in most cases longitudinal relaxation takes place via the one phonon process. The relaxation rate of this so-called direct process for tunneling states with two levels is given by[28]

$$\tau_d^{-1}=\left[\frac{\gamma_l^2}{v_l^5}+2\frac{\gamma_t^2}{v_t^5}\right]\frac{\Delta_0^2E}{2\pi\rho\hbar^4}\coth\left[\frac{E}{2k_BT}\right] \tag{13}$$

where ρ is the mass density, γ_i and v_i the elastic deformation potentials and the velocity of sound for longitudinal and transverse phonons, respectively. In $(KBr)_{1-x}(KCN)_x$ samples with CN^- concentrations of the order of a few percent, however, collective relaxation processes within small clusters of interacting tunneling systems are also important.[29,30] The temperature dependence of the relaxation rate of such processes is rather unusual, as the rate decreases with increasing temperature.[31]

The transverse relaxation time τ_2 is the time during which coherence of the resonant systems is preserved. It is limited by longitudinal relaxation and by processes that affect the phase of the precessing tunneling states. This situation can be expressed by $\tau_2^{-1}=\tau_1^{-1}/2+\tau_\phi^{-1}$ in which a phase memory time τ_ϕ is introduced. The origin of τ_ϕ is the mutual interaction of the tunneling states. One process well known in magnetic resonance[32] is the mutual flipping of systems of the same energy, called spin diffusion. In glasses, however, the density of tunneling states in resonance with the applied field is too dilute for this process to dominate dephasing. Here a more efficient dephasing mechanism, spectral diffusion becomes important. It is caused by the interaction of nonresonant, but thermally activated tunneling states with the resonant systems.[24-26] In the short time limit of this process, where the τ_1 of the nonresonant systems are longer than the duration of the echo experiment, a nonexponential decay of the echo is expected and a temperature dependence of the phase memory time $\tau_\phi\propto T^{-2}$. Indeed, due to this process, the temperature dependence of τ_2 in pure structural glasses is $\tau_2\propto T^{-2}$.[33] Situations in which the short time limit does not apply have been investigated[34] and in these regimes more complex decay patterns are predicted.

The previously described coherent behavior can only be studied if the time scale of the experiment is shorter than or of the order of the relaxation times τ_1 and τ_2. If $\Omega_R>\tau_1^{-1},\tau_2^{-1}$, the Bloch equations (10)–(12) can be solved analytically[35]

$$S_x=S_x^0\frac{1}{\Omega^2}[\Omega_R^2e^{-\alpha t}+\omega_d^2e^{-\beta t}\cos(\Omega t)]-S_y^0\frac{\omega_d}{\Omega}e^{-\beta t}\sin(\Omega t)+S_z^0\frac{\omega_d\Omega_R}{\Omega^2}[e^{-\beta t}\cos(\Omega t)-e^{-\alpha t}]+\frac{S_z^{\rm th}\Omega_R\omega_d}{\tau_1\alpha\Omega^2}[e^{-\alpha t}-1]\ , \tag{14}$$

$$S_y=S_x^0\frac{\omega_d}{\Omega}e^{-\beta t}\sin(\Omega t)+S_y^0e^{-\beta t}\cos(\Omega t)+S_z^0\frac{\Omega_R}{\Omega}e^{-\beta t}\sin(\Omega t)+\frac{S_z^{\rm th}\Omega_R}{\tau_1\Omega}\left[\frac{1}{\alpha\tau_2}+e^{-\alpha t}\left[1-\frac{1}{\alpha\tau_2}\right]-e^{-\beta t}\cos(\Omega t)\right]\ , \tag{15}$$

$$S_z=S_x^0\frac{\omega_d\Omega_R}{\Omega^2}[e^{-\beta t}\cos(\Omega t)-e^{-\alpha t}]-S_y^0\frac{\Omega_R}{\Omega}e^{-\beta t}\sin(\Omega t)+S_z^0\frac{1}{\Omega^2}[\omega_d^2e^{-\alpha t}+\Omega_R^2e^{-\beta t}\cos(\Omega t)]$$
$$+\frac{S_z^{\rm th}}{\tau_1\Omega^2}\left[\frac{\omega_d^2}{\alpha}(1-e^{-\alpha t})+\frac{\Omega_R^2}{\Omega}e^{-\beta t}\sin(\Omega t)\right]\ , \tag{16}$$

with abbreviations:

$$\alpha=\frac{1}{\Omega^2}\left[\frac{\omega_d^2}{\tau_1}+\frac{\Omega_R^2}{\tau_2}\right],\quad \beta=\frac{1}{\Omega^2}\left[\frac{\omega_d^2}{\tau_2}+\frac{\Omega_R^2}{2\tau_1}+\frac{\Omega_R^2}{2\tau_2}\right].$$

S_i^0 denotes the components of **S** at $t=0$ before the external field is applied. $\omega_d=\omega-\omega_r$ is the difference between the frequency of the applied field and the resonance frequency of the tunneling system, and $\Omega=(\Omega_R^2+\omega_d^2)^{1/2}$ is the effective Rabi frequency. These rather complex looking solutions can be simplified significantly in many cases. For example in rotary echo experiments with phase reversal of the external field at $t=t_p$ (see Sec. IV), we have $S_x^0=S_y^0=0$ and $S_z^0=-1$. If furthermore we only consider terms contributing to the rotary echo, its amplitude is being given by

$$A_r(t) \propto \int_0^{+\infty} \int_0^E P(E,\Delta_0) \frac{\Delta_0}{E} \frac{\mathbf{p}\cdot\mathbf{F}}{|\mathbf{F}|} \left[\frac{\Omega_R}{\Omega}\right]^3 e^{-\beta t} \times \sin[\Omega(t-2t_p)] d\Delta_0 dE \ . \quad (17)$$

$P(E,\Delta_0)$ denotes the distribution function. In general, the dipole moment and the angle θ between orientation of the dipole moment and the direction of the applied field may also be distributed and have to be taken into account. In glasses, rotary echo experiments[36] have been successfully described using an isotropic distribution of θ, a Gaussian distribution of the dipole moment, and a distribution of Δ_0 and E according to the tunneling model[16,17]

$$P(E,\Delta_0) dE\, d\Delta_0 = \bar{P} \frac{E}{\Delta_0} \frac{1}{\sqrt{E^2-\Delta_0^2}} dE\, d\Delta_0 \ , \quad (18)$$

where $\bar{P}$ is a material dependent constant. One central question of this work was to find out to what extent concentrated $(KBr)_{1-x}(KCN)_x$ samples have similar distributions of the quantities Δ_0 and E.

III. EXPERIMENTAL TECHNIQUE

As discussed in Sec II, a significant population difference is necessary in order to obtain a detectable echo amplitude. Furthermore, in order to study the temperature dependence of τ_1 and τ_2, a sufficiently large temperature range must be available for the experiment. Therefore, at our measuring frequency of 800 MHz, cooling of the samples to temperatures around 10 mK was necessary. Consequently, all experiments were performed in a ^{3}He-^{4}He dilution refrigerator. The cooling power of this apparatus is sufficient to overcome the heat input by the two coaxial cables carrying the rf signals and by the rf power dissipated in the experiment itself. All rf lines inside the refrigerator are semirigid coaxial cables with a low insertion loss up into the GHz range. Inside the vacuum enclosure of the refrigerator the coaxial cables are made from superconducting niobium in order to keep the heat input by thermal conduction as low as possible. Thermalization of the niobium cables is performed at the still ($\simeq$0.7 K) with custom-made stripline devices on a single-crystal sapphire substrate.

The echo experiments were performed in a reentrant microwave resonator screwed to the mixing chamber of the refrigerator with a low-pitch thread in order to improve thermal contact. The resonator is made from gold-plated oxygen-free copper. The samples,[37] disks with a thickness of 2 mm and a diameter of about 1 cm were mounted in the region between the center post and the bottom of the resonator. In this area, a large portion of the electric-field component of the resonator is concentrated and, because of the diameter of the center post (15 mm), the field is rather homogeneous. The bottom of the resonator is movable and pressed against the mixing chamber in order to ensure good thermal contact with both sides of the sample.

The rf signal is coupled into the resonator by a loop at the end of a short piece of semirigid coaxial cable. The loop can be rotated in order to adjust the degree of coupling. Heat transfer from the coaxial cables to the resonator and the sample is much reduced by a teflon bushing between the resonator wall and the coaxial cable. In most experiments the coupling was adjusted to an overcoupled condition keeping the Q factor of the resonator low ($Q \approx 150$) thus allowing experiments with high time resolution.

In nonlinear phenomena like the echoes we have investigated, knowledge of the absolute field amplitude in the sample is of importance. Therefore, for each experiment, the rf amplitude transmitted to the sample was measured outside the cryostat with a rf power meter, and the loss in the cables inside the cryostat was taken into account separately. In order to determine the amplitude inside the cavity, a second weakly coupled small loop was installed. With this loop a relative measure of the field amplitude could be obtained even during the experiment by simply measuring the rf amplitude at this loop. For a link of this value with an absolute measurement of the field amplitude, the coupling of the big loop was adjusted for critical coupling after the experiment. Under this condition all rf power is coupled into the cavity and the stored rf energy is, therefore, known. For an assessment of the field strength in the sample, the perturbation technique was employed. To this purpose two samples of the same material and of identical dimension were prepared, one of which (sample 2) had a 2-mm hole in the center. Perturbation theory associates the change $\delta\omega$ of the resonant frequency ω of the cavity with the change of rf energy in the sample relative to that in the whole resonator

$$\frac{\delta\omega}{\omega} \approx \frac{\int_{\text{sample 1}} \varepsilon_0(\varepsilon_r-1)F^2 dV - \int_{\text{sample 2}} \varepsilon_0(\varepsilon_r-1)F^2 dV}{2\int_{\text{cavity}} \varepsilon_0\varepsilon_r F^2 dV} \approx -\frac{\int_{\text{hole}} \varepsilon_r F^2 dV}{2\int_{\text{cavity}} \varepsilon_0\varepsilon_r F^2 dV} \ , \quad (19)$$

where F is the electric field and ε_r the dielectric constant in the sample. On the other hand, the denominator in Eq. (19) can also be expressed by the energy stored in the resonator with Q-factor Q

$$2\int_{\text{cavity}} \varepsilon_0\varepsilon_r F^2 dV \approx \frac{1}{\omega\varepsilon_0} P_{\text{rf}} Q \ , \quad (20)$$

where P_{rf} is the microwave power coupled into the resonator. If the field F in the sample is assumed to be homogeneous, the electric field in the hole—and thus in the whole sample—is given by

$$F \simeq \left[\delta\omega \frac{P_{\text{rf}} Q}{\varepsilon_0\varepsilon_r\omega^2 V_{\text{hole}}}\right]^{1/2} . \quad (21)$$

Using this method, the electric-field amplitude in the sample could be determined to an accuracy of 20%.

Let us now turn to the electronic circuitry necessary to generate and detect dielectric echo phenomena. An

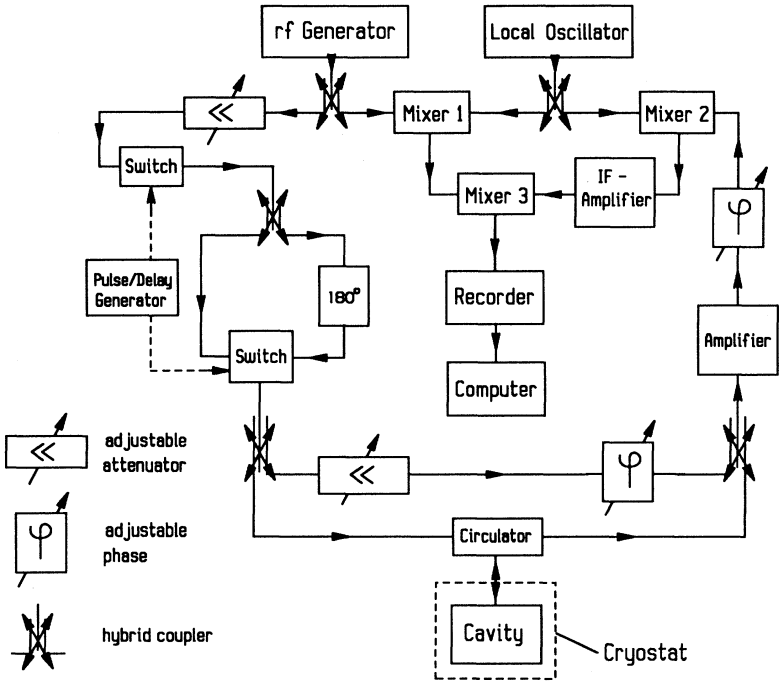

FIG. 1. Experimental setup for the generation and phase-sensitive detection of dielectric echoes.

overall schematic is shown in Fig. 1. The electronic system had to fulfill several demands: On the transmitter side it had to deliver rf pulses with duration ranging from 0.1 to 100 μs, and with peak powers between 10 dBm (10 mW) and -40 dBm (10^{-7} W). Furthermore, the phase of these pulses had to be switchable by 180° within the duration of a pulse in less than 1 μs.

The rf signal was produced by a microwave synthesizer (Rohde & Schwarz SMH). High-frequency stability of the rf signal is necessary for our experiment because of the phase-sensitive detection in the receiver, which will be discussed later. After the generator the signal is split between the receiver and the transmitter branch. In order to achieve the power level demanded by the experiment, the power divider was followed by a variable attenuator. The pulse shape of the rf signal was produced by a *p-i-n* diode switch with an on-off transit time of about 15 ns.

After the pulse shaping diode switch, the signal was split again, and a delay corresponding to a phase shift of 180° was introduced into one branch. By changing the position of the following double throw *p-i-n* diode switch, the signal could be phase inverted within less than 1 μs. Both *p-i-n* diode switches received their control signals from a four-channel digital delay generator with a resolution of 10 ns (Systron Donner 604).

From the double throw diode switch the signal was fed to another power divider and from there through a circulator into the cryostat and the resonator cavity. The purpose of the circulator was to provide a unidirectional power flow from the transmitter circuitry into the resonator and from there into the receiver branch thus improving the receiver sensitivity by 3 dB. The circuitry consisting of a phase shifter, a continuously variable attenuator, and the power dividers in the transmitter and the receiver branch forms a microwave bridge circuit. If attenuation and phase are properly adjusted, the signal reflected from the resonator because of nonperfect matching conditions can be cancelled. Therefore, only signal components originating from nonlinear phenomena (and, unfortunately, transients from the exponentially increasing or decreasing field amplitude in the resonator after switching) will appear at the receiver input.

The components following the microwave bridge form the receiver system. First, a broadband rf preamplifier with a gain of 20 dB and a noise figure of 1dB raises the signal level. The receiver is a superheterodyne system with an intermediate frequency of 60 MHz and a bandwidth of 10 MHz. The local oscillator (a Marconi Instruments 6070A cavity oscillator) drives two mixers, mixer 1 producing the intermediate frequency for the i.f. amplifier and mixer 2 generating a 60-MHz phase reference by mixing a sample of the rf generator output with that of the local oscillator. Finally, mixer 3 works as a phase-sensitive demodulator by mixing the output of the i.f. amplifier with the phase reference. After the preamplifier a phase shifter allows one to adjust the signal phase so that maximum signal amplitude is obtained at the demodulator. The mixer is followed by a 100-MHz transient recorder (Biomation 8100) and a personal computer that adds up subsequent echo cycles and thus performs signal averaging. Between 100 and 1000 averaging cycles were necessary to reach an acceptable signal-to-noise ratio in our experiments. Including the signal-to-noise improvement by averaging, the sensitivity of our receiving system was better than 10^{-16} W.

Phase-sensitive detection has two advantages for our experiment. First, sensitivity is increased by 3 dB because all noise in the quadrature component of the signal is suppressed. Second, the output of a phase-sensitive

detector is bipolar. Therefore, the noise in the detector signal will have a mean value of zero. In a conventional rectifying (square law) detector the noise output is unipolar and will, therefore, average to a finite value. Furthermore, mixing of the bipolar random noise signal with the fixed-polarity echo signal in a rectifying detector would lead to a nonlinear amplitude dependence of the averaged echo signal at low amplitudes.

IV. ROTARY ECHOES

The formation of a rotary echo is schematically illustrated in Fig. 2. At low temperatures ($k_B T < \hbar\omega_r$) the majority of the resonant tunneling system is in the ground state. According to Eq. (8) their occupation number difference δN starts to oscillate at the Rabi frequency when an external rf field is applied and consequently their electrical polarization will oscillate as well. If tunneling systems with different Rabi frequencies contribute to the signal, the resulting macroscopic polarization vanishes rapidly because of superposition of the individual contributions. In many cases it is impossible to detect the polarization of the sample at the beginning of the pulse sequence because the amplifiers are saturated for a few μs after switching on the rf signal. But since a phase inversion of the driving field at $t = t_p$ is equivalent to a reversal of time evolution of the polarization, the Rabi oscillations will appear again around $t = 2t_p$. This phenomenon is called the rotary echo.

The duration of the echo, or more precisely, the number of visible cycles, is determined by the distribution of the effective Rabi frequencies Ω. Since the energy of the contributing tunneling states $E = \hbar\omega_r$ is fixed within the bandwidth of the microwave resonator and the electrical-field amplitude $\mathbf{F}_0$ is set by the external field, a distribution of the effective Rabi frequency Ω is mainly due to a distribution of the tunnel splittings Δ_0 or of the dipole moment $\mathbf{p}$. Therefore, rotary echo experiments are a suitable tool to study the distribution of these parameters. For example, in amorphous materials only one cycle is visible in the rotary echo, which, above all, is due to the broad distribution of their tunnel splittings Δ_0.[36]

Figure 3 shows a typical signal pattern of a rotary echo observed in $(KBr)_{0.95}(KCN)_{0.05}$. The phase of the rf field was reversed at $t = 6$ μs and the echo is centered at $t = 12$ μs. This signal has a number of interesting features that will be discussed in the following. First of all, the rotary echo extends over more than 8 μs and shows about 10 clearly visible cycles, indicating that the underlying distribution of both, Δ_0 and $\mathbf{p}$ is rather narrow. As a further consequence of their long duration, the Rabi oscillations are also detectable before the phase inversion in this particular system. In addition to these more or less expected features, a slowly decaying polarization background appears in the signal before and after the phase inversion at t_p. We believe that it is not caused by experimental artifacts, since it was present in all rotary echo experiments on $(KBr)_{1-x}(KCN)_x$ and did not appear in rotary echoes observed with the same apparatus in glasses.[36] We rather think that the polarization background as well is caused by the dynamical properties of the tunneling states in $(KBr)_{1-x}(KCN)_x$. A possible mechanism will be discussed at the end of this section.

Let us now discuss the main result of our rotary echo experiments in $(KBr)_{1-x}(KCN)_x$, namely the distribution of the effective Rabi frequencies. For a more quantitative analysis of our echo data and to display the distribution of effective Rabi frequencies, the rotary echo data were Fourier transformed. In order to avoid contributions

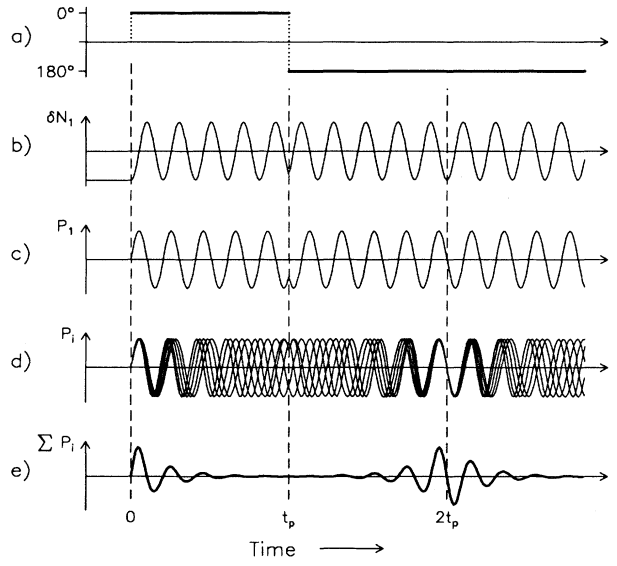

FIG. 2. Formation of a dielectric rotary echo. (a) Phase of the applied rf field, (b) time evolution of the occupation number difference of the two levels of an ensemble of identical tunneling states, (c) time evolution of the corresponding electrical polarization, (d) superposition of the polarization of five tunneling systems with slightly different Rabi frequencies, and (e) time evolution of the resulting macroscopic polarization of tunneling systems with a Lorentzian distribution of Rabi frequencies.

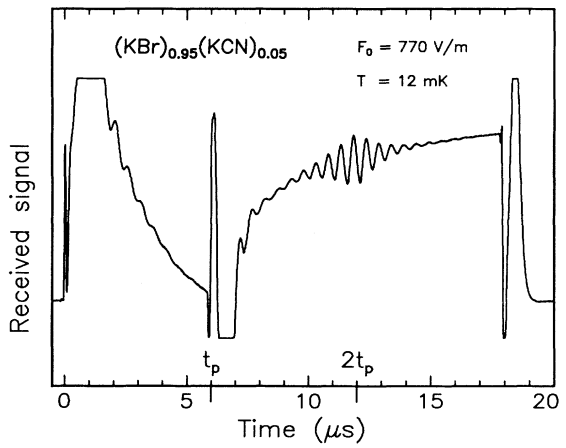

FIG. 3. Typical signal pattern of a rotary echo experiment in $(KBr)_{0.95}(KCN)_{0.05}$ at 12 mK. The phase of the applied rf field was reversed at $t = 6$ μs. The rotary echo extends from $t \simeq 8$–16 μs.

from the slowly decaying polarization background, it was subtracted numerically before carrying out the Fourier transformation. The rotary echo data of a $(KBr)_{0.95}(KCN)_{0.05}$ crystal prepared in this way and the corresponding Fourier spectrum are shown in Fig. 4. The slightly asymmetric shape of the echo envelope is a consequence of phase decay with $\tau_2 \simeq 4$ μs (see Sec. V). For a direct comparison of the results obtained for different samples, all Fourier spectra have been normalized relative to the amplitude and the frequency at the maximum.

In order to evaluate the distribution of Δ_0 and E, we have fitted the echo signal using Eq. (17). Since the distribution of the effective Rabi frequencies is relatively narrow in the case of $(KBr)_{0.95}(KCN)_{0.05}$ we have used in our calculations a fixed value for the dipole moment $|\mathbf{p}|$ and its angle θ with the applied field. We should point out that it is not possible to distinguish between a distribution of Δ_0 or $\mathbf{p}$ in our experiment. Therefore, Δ_0 might have even been distributed slightly narrower than obtained from our fitting procedure.

Surprisingly, the quantitative analysis of our data shows that only systems with a well-defined energy E contribute to the rotary echo amplitude in $(KBr)_{0.95}(KCN)_{0.05}$. Their resonance frequency ω_r is identical with the frequency ω of the external rf field, and hence $\omega_d = 0$. At first glance this result seems unreasonable, because Δ and thus the energy $E = \hbar\omega_r$ are known to be broadly distributed in $(KBr)_{1-x}(KCN)_x$ samples containing a few percent of CN^-.[4,29] Consequently, one would expect that all systems with resonance frequencies within the bandwidth of the cavity contribute to the echo. The reason why this is not the case for $(KBr)_{0.95}(KCN)_{0.05}$ can be understood by discussing the influence of spectral diffusion in rotary echo experiments. Spectral diffusion is due to longitudinal interaction with thermally fluctuating tunneling states. Since this coupling is proportional to their asymmetry energy Δ, the influence of spectral diffusion onto the effective Rabi frequency $\Omega = (\Omega_R^2 + \omega_d^2)^{1/2}$ can be estimated from the derivative $d\Omega/d\Delta$,

$$\frac{d\Omega}{d\Delta} = \frac{1}{\Omega}\left[\frac{\Delta}{E}\frac{\omega_d}{\hbar} - \Omega_R^2\frac{\Delta}{E^2}\right] . \tag{22}$$

This expression is minimal (zero) in two cases: for systems without asymmetry, i.e., for $\Delta = 0$ and for those with $\omega_d = (\hbar\Omega_R/E)\Omega_R$. Since the factor $\hbar\Omega_R/E$ is typically of the order of 10^{-3}–10^{-4}, spectral diffusion is not important for systems with $\omega_d \ll \Omega_R$. States with $\omega_d/\Omega_R \gg 0$, however, rapidly lose phase coherence and thus cannot contribute to the rotary echo. This explains why exclusively systems with resonance frequencies close to the frequency of the applied field are observed in our experiment. Figure 5 shows a plot of Eq. (22) as a function of ω_d/Ω_R with parameters typical for our experiment. Clearly, the influence of spectral diffusion is strongly reduced for systems with $|\omega_d| \ll \Omega_R$, confirming the observation that in $(KBr)_{1-x}(KCN)_x$ only systems with resonance frequencies corresponding to the frequency of the external rf signal contribute to the echo.[38]

Because of this effect it was justified to keep not only the values of $|\mathbf{p}|$ and θ, but also the energy splitting E constant in our numerical calculation of the distribution of the effective Rabi frequencies. Thus the distribution of the Rabi frequencies directly reflects the distribution of the tunnel splitting Δ_0, for which we assumed a Lorentz distribution,

$$P(\Delta_0)d\Delta_0 = \frac{1}{2\pi}\frac{1}{(\Delta_0 - \bar{\Delta}_0)^2 + (\xi/2)^2}d\Delta_0 . \tag{23}$$

ξ denotes the width of the Lorentz distribution and $\bar{\Delta}_0$ the mean value of the tunnel splitting. According to measurements of the dielectric constant.[39] $\bar{\Delta}_0/k_B$ is of the order of 10 mK. Figures 4, 6, and 7 show the results of rotary echo experiments on $(KBr)_{1-x}(KCN)_x$ samples

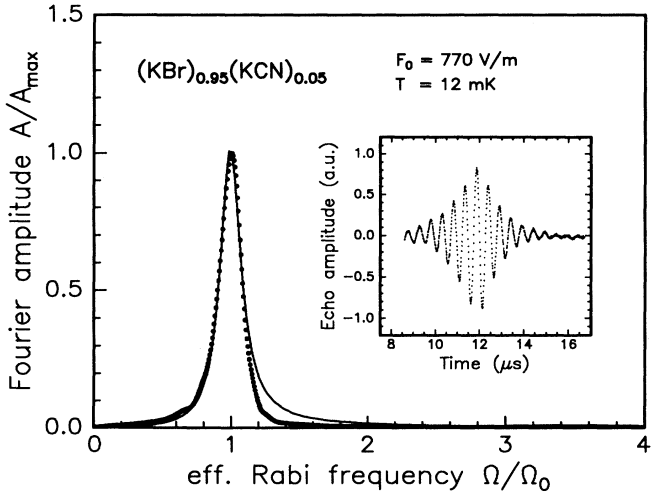

FIG. 4. Fourier transformation of the amplitude of a rotary echo in $(KBr)_{0.95}(KCN)_{0.05}$. The solid line represents a numerical fit with a Lorentzian distribution of Δ_0. The insert shows the rotary echo data used for the Fourier transformation.

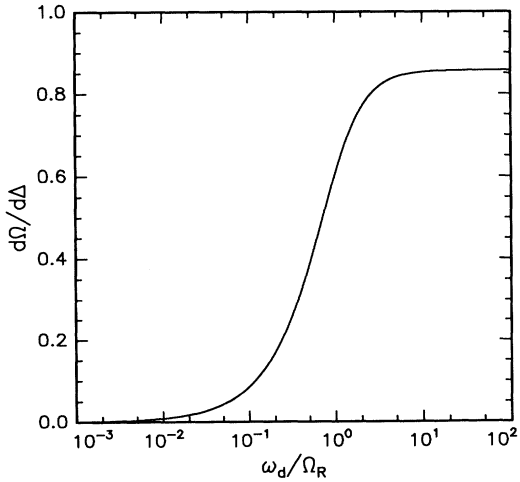

FIG. 5. Derivative of the effective Rabi frequency Ω with respect to the asymmetry energy Δ as a function of ω_d/Ω_R.

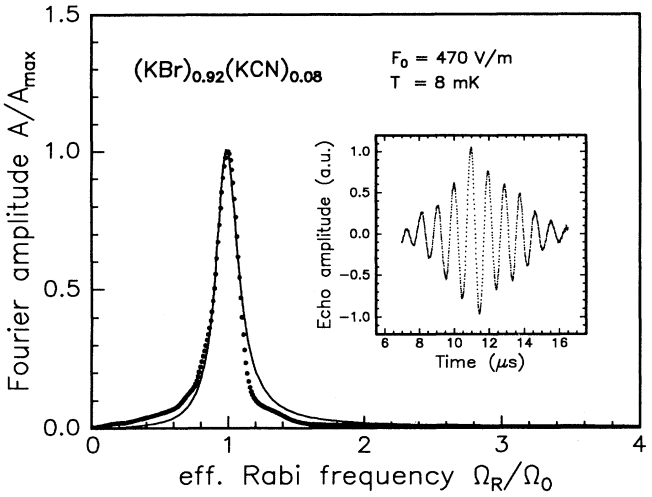

FIG. 6. Fourier transformation of the amplitude of a rotary echo in $(KBr)_{0.92}(KCN)_{0.08}$. The solid line represents a numerical fit with a Lorentz distribution of Δ_0. The insert shows the rotary echo data used for the Fourier transformation.

with $x=0.05$, 0.08, and 0.18 and the corresponding distribution of the effective Rabi frequencies. The solid lines represent fits with the assumptions described above. The width of the distribution ξ is 1.8, 2, and 4.5 mK for the samples with $x=0.05$, 0.08, and 0.18, respectively. Taking into account that no other parameter was allowed to be distributed in our calculation, these values represent an upper limit for the width ξ. It increases with concentration of CN^- as one would expect, but it is still relatively small for the sample with $x=0.18$. This result shows that the interpretation of previous experiments for a sample with $x=0.2$ (Ref. 20) was not correct, where a glasslike distribution of the tunneling parameters was suggested from the data available at that time. In Fig. 7 the distribution of the effective Rabi frequencies of $(KBr)_{0.82}(KCN)_{0.18}$ is compared with that for the structural glass Suprasil W. The curve for the glass sample is clearly much broader than that for $(KBr)_{0.82}(KCN)_{0.18}$. We, therefore, conclude that the distribution of the fundamental parameters of the tunneling states for $(KBr)_{1-x}(KCN)_x$ differs considerably from that of amorphous materials, although in many aspects $(KBr)_{1-x}(KCN)_x$ shows a low-temperature behavior typical for a glass.

The fact that Δ_0 is hardly distributed in the $(KBr)_{1-x}(KCN)_x$ samples investigated, is remarkable in another sense as well. It shows that the echoes are associated with a well-defined species of tunneling states. Nevertheless, they cannot be isolated CN^- molecules, since the tunnel splitting Δ_0^i/k_B of those is about 1 K. Most likely the additional excitations with a small discrete energy splitting are caused by strongly interacting neighboring tunneling states. A coarse estimate of the tunnel splitting of such coupled states can be obtained from the spectrum of a pair of coupled two-level systems.[21] The two lowest levels of the resulting four-level system are separated by $(\Delta_0^i)^2/J$, where J is the coupling energy. With our value of $\Delta_0/k_B \simeq 10$ mK and $\Delta_0^i/k_B \simeq 1$ K, one finds $J/k_B \simeq 100$ K. Assuming elastic quadrupole interaction such a high value for J indicates that the coupled states are formed by pairs of next-neighbor CN^- molecules.[40]

According to Eq. (9) the frequency of the maximum of the Fourier spectrum should vary linearly with the amplitude of the applied field. As shown in Fig. 8 this dependence could be nicely demonstrated for three different $(KBr)_{1-x}(KCN)_x$ samples over more than a decade in

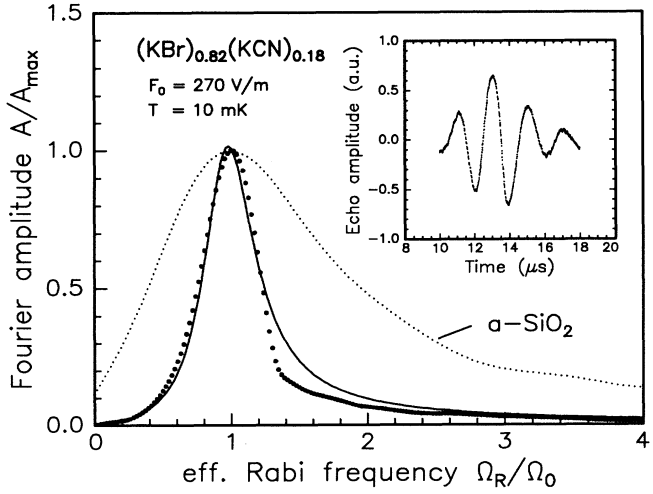

FIG. 7. Fourier transformation of the amplitude of a rotary echo in $(KBr)_{0.82}(KCN)_{0.18}$. The solid line represents a numerical fit with a Lorentz distribution of Δ_0. The subplot shows the rotary echo data used for the Fourier transformation. The dotted line is the Fourier transformation of a rotary echo in vitreous silica (Suprasil W) (Ref. 36).

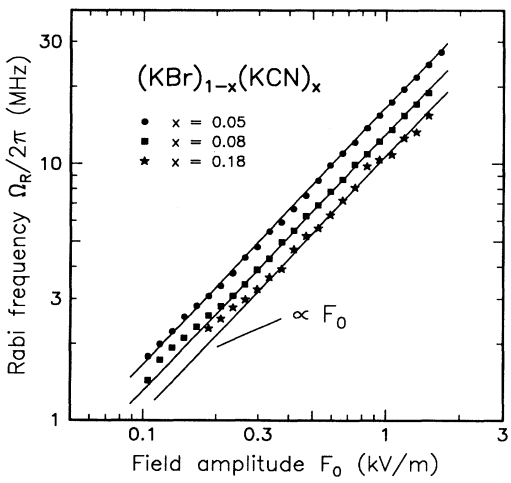

FIG. 8. Double logarithmic plot of the Rabi frequencies Ω_R as a function of the electrical-field strength F_0 (local field) for samples with three different CN^- concentrations. In agreement with Eq. (9) the Rabi frequency depends linearly on F_0.

field amplitude. From these curves the effective dipole moment $(\Delta_0/E)|\mathbf{p}|$ of the resonant tunneling states can be estimated. Taking into account local-field corrections we find 0.56 D for $x=0.05$, 0.4 D for $x=0.08$ and 0.3 D for $x=0.18$. Although the statistical error is small, the uncertainty is rather large because of the difficulties in the determination of the electrical-field strength in the sample, as discussed in Sec. III. The overall uncertainty is of the order of 20%. Therefore, we cannot definitely state that we have observed a concentration dependence of the dipole moment. Although the resonant tunneling states in our experiment can clearly not be isolated CN^- molecules, it is interesting to note that the dipole moment of CN^- tunneling states in very dilute samples has been measured to be of the order of 0.5 D.[41]

Let us now come back to the slowly decaying background signal observed in all $(KBr)_{1-x}(KCN)_x$ samples, but not in glasses. It can be attributed to tunneling systems, that differ from the states contributing to the echoes only by the fact that they have no asymmetry Δ. Therefore, their energy is exclusively determined by the tunnel splitting $\Delta_0/k_B \simeq 10$ mK $\hat{=}$ 200 MHz. Their phase relaxation time must be extremely short ($\tau_2 \simeq 10$ ns) whereas their longitudinal relaxation time τ_1 must be of the order of 50 μs. The presence of such tunneling states in $(KBr)_{1-x}(KCN)_x$ has been concluded from measurements of the low-temperature dielectric constant of samples with concentrations $x=0.001$ and $x=0.01$.[39] Although these systems are far off-resonance, a weak interaction with the applied field takes place because of their large linewidth τ_2^{-1}. Therefore, an absorption occurs, which saturates after about 20 μs. With the above parameters the observed behavior can be well described by the Bloch equations. To support our interpretation we performed a double-pulse experiment with two pulses with a duration of 5 μs and with variable spacing. For the second pulse the amplitude of the slowly varying background is reduced. With increasing delay it recovers because those systems that have relaxed to the ground state now can contribute to the absorption again. This experiment has also directly confirmed the value of τ_1 assumed in the calculations.

In addition, it should be noted that the slowly decaying background has also been observed in echo experiments on samples with $x=0.001$ and $x=0.01$, however it was not possible to detect any coherent echoes. This is remarkable since echoes could be observed in samples with both higher and lower CN^- concentration.[19] We can only presume that an extremely fast dephasing of the resonant states in the samples with $x=0.001$ and $x=0.01$ is the reason for the unsuccessful echo experiments.

V. TWO-PULSE ECHO EXPERIMENTS

In order to investigate the transverse relaxation time τ_2 we carried out two-pulse echo experiments. The tunneling states are in thermal equilibrium at the beginning of the pulse sequence and hence the components of $\mathbf{S}$ are $S_z^0=S_y^0=0$ and $S_z^0=-1$. According to Eq. (6)–(8) the first pulse, adjusted in amplitude and duration to fulfill the condition $\Omega_R t=\pi/2$, turns $\mathbf{S}$ into the x,y plane, leading to a macroscopic polarization. Due to the distribution of the resonance frequencies the vectors $\mathbf{S}_j$ of the individual tunneling systems rotate at different speed. The macroscopic polarization vanishes after a certain time because the vectors $\mathbf{S}_j$ become uniformly distributed in the x,y plane. This process is analogous to the well-known free-induction decay in magnetic-resonance experiments.[32] After a short delay $t=t_{12}$ a second pulse fulfilling $\Omega_R t=\pi$ is applied, leading to a counter-rotation of each individual $\mathbf{S}_j$. This situation is equivalent to a reversal of the time evolution of each $\mathbf{S}_j$. Consequently, at $t=2t_{12}$ all $\mathbf{S}_j$ superimpose constructively again and a macroscopic polarization appears, the spontaneous echo. Figure 9 shows a typical signal pattern for a $\pi/2$, π pulse sequence in a $(KBr)_{0.95}(KCN)_{0.05}$ sample at 12 mK. In this case the delay time t_{12} was 5 μs and the width of the pulses was 250 ns for the first and 500 ns for the second pulse. In Fig. 9 the recorded pulses appear much broader because the large signals of the excitation pulses saturate the receiver for about 1 μs. After 10 μs the spontaneous echo appears.

As discussed in Sec. II only systems that have not undergone phase disturbing processes contribute to the echo. Therefore, the amplitude of the echo depends on the delay time t_{12}. In the simplest case, an exponential decay with the delay time is found and the maximum amplitude $A_2(2t_{12})$ of the two-pulse echo as a function of the delay time is given by

$$A_2(2t_{12})=A_2^0 e^{-2t_{12}/\tau_2}. \tag{24}$$

The decay curves at different temperatures for the $(KBr)_{0.95}(KCN)_{0.05}$ sample are shown in Fig. 10. At all temperatures, except the lowest, we clearly find an exponential decay and, therefore, the transverse relaxation time can directly be derived from this experiment. The small deviations at $T=15$ mK are due to experimental problems. The temperature dependence of τ_2 for $(KBr)_{0.95}(KCN)_{0.05}$ is shown in Fig. 11. At the lowest

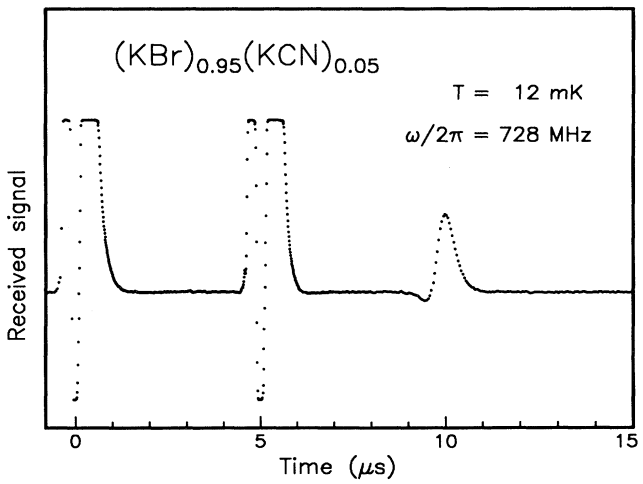

FIG. 9. Typical signal pattern of a two-pulse echo experiment on $(KBr)_{0.95}(KCN)_{0.05}$. The maximum amplitude of the echo appears at $t=10$ μs.

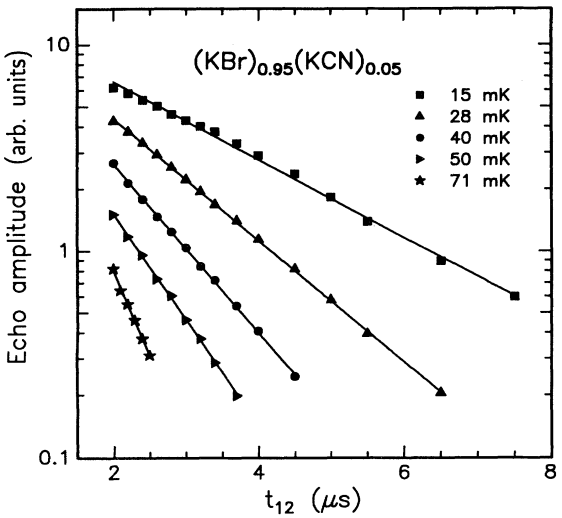

FIG. 10. Amplitude decay of the two-pulse echo in $(KBr)_{0.95}(KCN)_{0.05}$ as a function of pulse separation t_{12} and temperature. Data for different temperatures are offset vertically for clarity. Solid lines are fits according to Eq. (24).

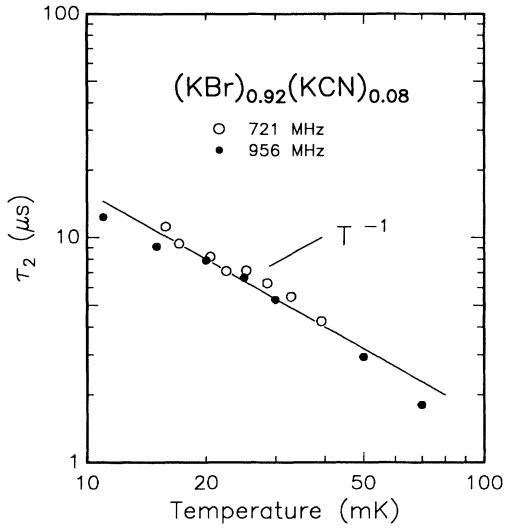

FIG. 12. Decay time of the two-pulse echo amplitude in $(KBr)_{0.92}(KCN)_{0.08}$ as a function of temperature. Data were taken at two different frequencies.

temperatures the value of τ_2 is 4 μs, which is smaller by about a factor of 5 compared to a structural glass (SiO_2). The temperature dependence is close to T^{-1} up to at least 90 mK, although a slight deviation from a power-law dependence is visible. Hence τ_2 does not follow the T^{-2} dependence predicted for spectral diffusion in glasses.[24] It should be stated, however, that similar experiments in glasses have also resulted in temperature dependencies for τ_2 ranging from T^{-1} to T^{-2}.[33,36,42]

The data of τ_2 for $(KBr)_{0.92}(KCN)_{0.08}$ are shown in Fig. 12. In this case, the relaxation time is a factor of 2 longer than in $(KBr)_{0.95}(KCN)_{0.05}$, but the temperature dependence is the same. The data of the decay time for $(KBr)_{0.92}(KCN)_{0.08}$ were obtained at slightly different frequencies. Within the experimental error we find no significant frequency dependence. In order to explain the temperature dependence of τ_2 for both samples, the dominating dephasing mechanism, which can be either longitudinal relaxation (τ_1 processes) or phase relaxation due to interaction among tunneling states, must be known. Although, according to Eq. (13) the relaxation rate due to the one phonon process varies linearly with temperature for $\hbar\omega_r < k_B T$, this mechanism does not dominate the dephasing in $(KBr)_{1-x}(KCN)_x$ as we will show in the following section. Therefore, interaction between the tunneling states must be the cause of the dephasing. From this point of view, at first glance, the fact that the relaxation times are longer for the higher concentrated sample is surprising, but it is known from other experiments (e.g., specific-heat measurements[4]) that the density of states is lower for higher concentrated samples. Therefore, dephasing mechanisms that are due to the interaction among the tunneling states are less effective at higher concentrations. Presently, because of the lack of an adequate theory for the coherent properties of tunneling states in crystalline hosts, the results of our two-pulse echo experiments seem difficult to explain in more detail.

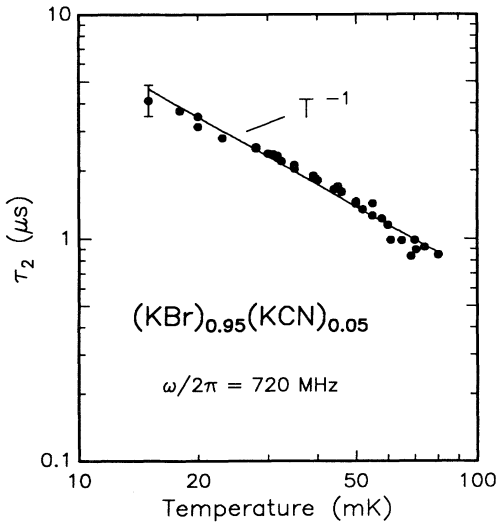

FIG. 11. Decay time of the two-pulse echo amplitude in $(KBr)_{0.95}(KCN)_{0.05}$ as a function of temperature.

Finally, we want to point out that our two-pulse echo data fit well with earlier echo measurements by Foote and Golding[19] on lower and higher concentrated $(KBr)_{1-x}(KCN)_x$ samples. One interesting difference, however, should be mentioned. Foote and Golding report nonexponential decays of the echo amplitude for a sample with $x=0.5$, whereas our data ($x=0.05$ and $x=0.08$) can be described using exponential decay curves.

VI. THREE-PULSE ECHO EXPERIMENTS

Two different types of three-pulse echo experiments, stimulated echoes and recovery echoes, were used to in-

vestigate the longitudinal dephasing mechanism. Let us first describe the experiments using stimulated echoes. The generation of this echo is somewhat more difficult to illustrate. An elaborate description of this phenomenon is given by Hahn.[43] The pulse sequence consists of three identical pulses with duration and amplitude adjusted to obtain $\Omega_r t=\pi/2$. In contrast to the situation in two-pulse echo experiments, the $\mathbf{S}_j$ vectors of the resonant tunneling states have a finite x component after the second pulse, corresponding to their individual position in the x,y plane at $t=t_{12}$ just before the second pulse. Therefore, this z component represents the phase difference between the tunneling states and the driving field at $t=t_{12}$. If in the following the z component is not changed due to inelastic processes, the third $\pi/2$ pulse will turn the $\mathbf{S}_j$ vectors again into the x,y plane, where the systems now will have y components opposite to those before the application of the second pulse. This situation is equivalent to a time reversal at $t=t_{12}$ and thus a macroscopic polarization, the stimulated echo, will appear at $t=t_{12}+t_{13}$. Obviously, by varying the delay time t_{13} between the first and the third pulse, the influence of longitudinal relaxation processes can be studied. For a single relaxation time τ_1 an exponential decay of the echo amplitude is expected,

$$A_3(t_{12}+t_{13})=A_3^0 e^{-(t_{12}+t_{13})/\tau_1} . \tag{25}$$

The decay curves of the amplitude of stimulated echoes in a $(KBr)_{0.92}(KCN)_{0.08}$ sample for different temperatures are shown in Fig. 13. At all temperatures we find a nonexponential decay, indicating that tunneling systems with a broad distribution of relaxation times contribute to this echo. Therefore, it is not possible to deduce τ_1 as a function of temperature from the decay curves. In general, the decay of the stimulated echo is much slower than that of the spontaneous echo. This shows that interaction among the tunneling states and not the one phonon relaxation dominate the transverse dephasing in this sample. Similar observations have been made for the samples with CN^- concentrations $x=0.05$ and $x=0.18$.

A simple method to prove the influence of spectral diffusion onto the dephasing is to vary the delay time t_{12} between the first two closely spaced pulses.[18] The envelope of the frequency spectrum of the first two pulses is comblike with a spacing of t_{12}^{-1}. After the second pulse this spectrum is preserved in the z component of $\mathbf{S}$. The comb will decay by energy relaxation processes and by frequency fluctuations due to spectral diffusion of the excited states over a considerable fraction of t_{12}^{-1}. Therefore, the importance of spectral diffusion will depend on the spacing of the first two pulses. The result of such a measurement with different t_{12} for $(KBr)_{0.92}(KCN)_{0.08}$ is shown Fig. 14. The rather strong dependence of the echo decay on t_{12} shows that spectral diffusion dominates the decay of the stimulated echo in this sample.

To avoid falsification of measurements of τ_1 of tunneling states by spectral diffusion, an alternative pulse sequence has been introduced by Golding *et al.*[44] In this case initially a π pulse is applied to invert the population of the two levels. In the following this population will relax back to its thermal equilibrium by energy relaxation processes. After a delay time t_{12} the recovery of the population is monitored using an ordinary two-pulse echo. For short delay times, because of the inversion, the observed echo will be "negative" and then will approach its normal amplitude with increasing t_{12}. In the simplest case, for a single relaxation time, the recovery of the spontaneous echo can be described by

$$A(t_{12}+t_{13})=A_3^0(1-2qe^{-(t_{12}+t_{13})/\tau_1}) . \tag{26}$$

The factor q denotes the degree of inversion, since com-

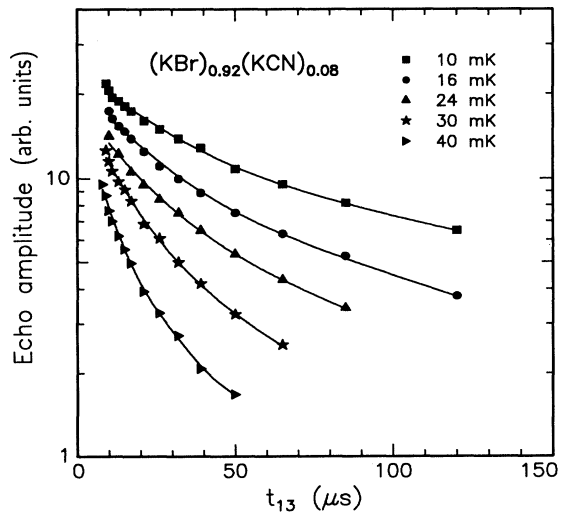

FIG. 13. Amplitude decay of the three-pulse echo in $(KBr)_{0.92}(KCN)_{0.08}$ as a function of pulse separation t_{13} and temperature. Curves are offset vertically for clarity. Solid lines through data sets are guides to the eye.

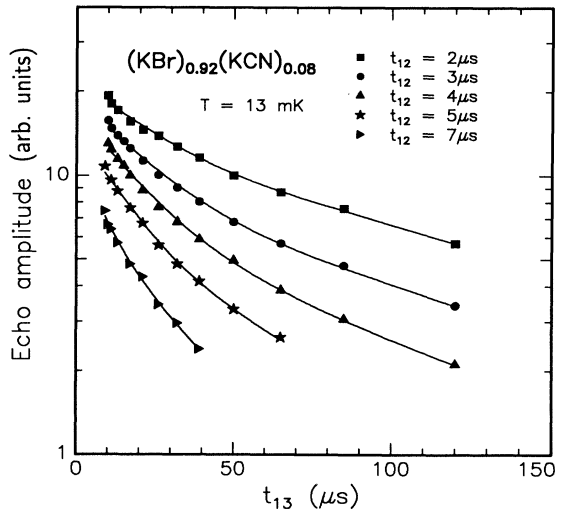

FIG. 14. Decay of the amplitude of stimulated echoes in $(KBr)_{0.92}(KCN)_{0.08}$ as a function of pulse separation t_{13} and of pulse separation t_{12}. Curves are offset vertically for clarity. Solid lines through data sets are guides to the eye.

plete inversion is impossible for an inhomogeneously broadened system. The recovery of the echo amplitude of a spontaneous echo after inversion in a $(KBr)_{0.92}(KCN)_{0.08}$ sample at $T=15$ mK is shown in Fig. 15. The dashed-dotted line is a fit according to Eq. (26) with $q=0.51$ and $\tau_1=250$ μs. The disagreement between fit and data at long delay times indicates that the relaxation times of the systems contributing to the signal are distributed. The same observation was made by Foote and Golding[19] for samples with both higher and lower defect concentration. The presence of this distribution is surprising considering the fact that we investigate states with rather well-defined tunneling parameters Δ_0, **p**, and E given by our experimental frequency. Corresponding recovery curves in $(KBr)_{0.92}(KCN)_{0.08}$ for temperatures between 10 and 50 mK were found to be nearly identical. This shows that the recovery time in $(KBr)_{0.92}(KCN)_{0.08}$ is almost independent of temperature below $T=50$ mK. Within the uncertainty of the fitting procedure we find for the initial recovery time a constant value $\tau_1\simeq(270\pm40)$ μs. Qualitatively, the situation for $(KBr)_{0.95}(KCN)_{0.05}$ is very similar, but the initial recovery time below 50 mK in this case is $\tau_1\simeq(80\pm10)$ μs. In contrast to that, the temperature dependence of the initial recovery time of the $(KBr)_{0.82}(KCN)_{0.18}$ sample is rather unusual (Fig. 16). With increasing temperature the initial recovery slows down considerably. It is interesting to note that Foote and Golding[19] observed a similar recovery behavior for a much lower concentrated sample ($x=0.000\,34$). Obviously, such a temperature dependence cannot be explained by the relaxation via thermal phonons. The phenomenon might be due to collective relaxation within small clusters of coupled CN^- molecules. Janssen has shown that collective relaxation processes have a relaxation rate that decreases with increasing temperature.[31] On the other hand, a phonon bottleneck effect with an initial avalanche decay as suggested by Foote and Golding[19] for $x=0.000\,34$ cannot be ruled out, although in our opinion the relatively high CN^- concentration of the $(KBr)_{0.92}(KCN)_{0.18}$ sample favors collective relaxation processes as a cause for this observation.

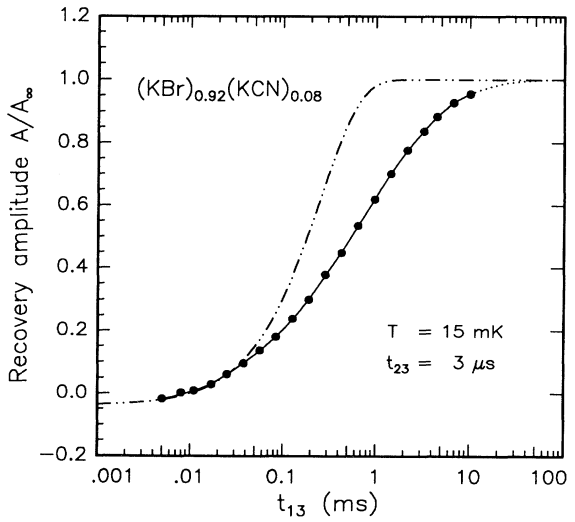

FIG. 15. Recovery of the echo amplitude of a spontaneous echo after inversion in $(KBr)_{0.92}(KCN)_{0.08}$ at $T=15$ mK normalized to the amplitude of a spontaneous echo without inversion. The dashed-dotted line represents an exponential recovery with a single relaxation time $\tau_1=250$ μs. The solid line is a guide to the eye.

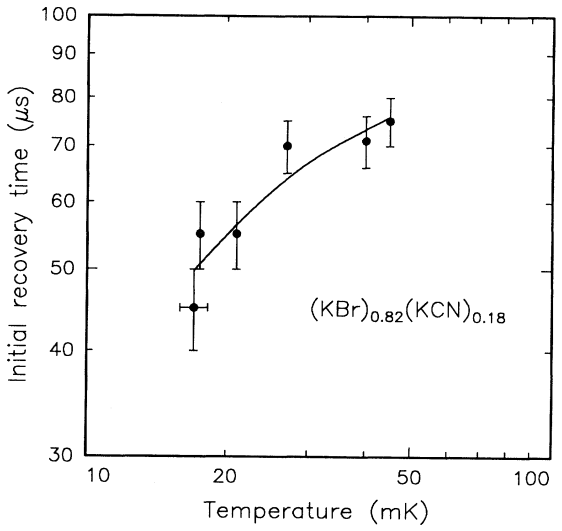

FIG. 16. Initial recovery time τ_1 of a spontaneous echo after inversion in $(KBr)_{0.82}(KCN)_{0.18}$ as a function of temperature. The solid line is a guide to the eye.

VII. SUMMARY

$(KBr)_{1-x}(KCN)_x$ crystals with CN^- concentrations between $x\simeq0.05$ and $x\simeq0.55$ freeze into an orientationally disordered phase at low temperatures. The low-temperature behavior of $(KBr)_{1-x}(KCN)_x$ crystals in the orientational glass state is dominated by atomic tunneling systems and many of their properties are very similar to those in structural glasses. Since the origin of the low-energy excitations in the case of $(KBr)_{1-x}(KCN)_x$ is known, this system has been discussed as a model system for the low-temperature anomalies of amorphous materials.

We have investigated the coherent dynamics of the atomic tunneling states in $(KBr)_{1-x}(KCN)_x$ samples with different CN^- concentration, ranging from $x=0.0001$ to $x=0.18$. Using rotary echo experiments the distribution of the effective Rabi frequencies has been measured. For all $(KBr)_{1-x}(KCN)_x$ samples investigated this distribution was found to be very narrow compared with that obtained for glasses in similar experiments. This shows that the distribution of the fundamental parameters of the tunneling states in $(KBr)_{1-x}(KCN)_x$ is quite different from that in glasses, at least up to a CN^- concentration of 18%.

The very narrow distribution of the tunnel splitting in $(KBr)_{1-x}(KCN)_x$ indicates that well-defined species of

tunneling systems dominate the coherent properties at frequencies of about 750 MHz. Since their corresponding energy splitting E/k_B is of the order of 35 mK, they are not associated with isolated CN^- molecules. The presence of these low-energy tunneling states can be explained by pairs of strongly coupled CN^- molecules. From the estimated value of the interaction energy we suppose that these pairs are formed by next-neighbor CN^- molecules. With rotary echoes we have measured the effective dipole moment $(\Delta_0/E)|\mathbf{p}|$ of the resonant states. We found values in the range from 0.3–0.6 D for all samples.

In addition, we have studied the decay of spontaneous and stimulated echoes in two- and three-pulse echo experiments. In both cases, the decay of the echo amplitude was clearly dominated by spectral diffusion, a process originating from interaction among the tunneling states. Although this mechanism determines the dephasing in glasses as well, significant differences in the time and temperature dependence were observed. The energy relaxation time τ_1 has been measured using the recovery of the spontaneous echoes after inversion. For all samples we found a distribution of τ_1, the origin of which is not yet understood. The temperature dependence of τ_1 for the sample with $x=0.18$ was found to be rather unusual, since it increased with temperature. Such a behavior can qualitatively be described by collective relaxation processes of interacting CN^- molecules.

In conclusion, we would like to state that our investigation shows that the coherent dynamics of the tunneling states in $(KBr)_{1-x}(KCN)_x$ are quite different from those in structural glasses. Although the origin of the tunneling states in $(KBr)_{1-x}(KCN)_x$ is known, a detailed and complete understanding of the dynamical properties of the low-energy excitations in this system is still lacking.

ACKNOWLEDGMENTS

We would like to thank S. Hunklinger, D. A. Parshin, G. Weiss, R. Weis, and A. Würger for many stimulating discussions and we are grateful to S. Haussühl for providing the samples.

*Present address: Laboratorium für Physikalische Chemie, ETH Zürich, Universitäts-Str. 22, 8092 Zürich, Switzerland.
†Present address: Institut für Technische Physik, Universität des Saarlands, Im Stadtwald 38, 66041 Saarbrücken, Germany.

[1]F. Lüty, in *Defects in Insulating Crystals,* edited by V. M. Turkevich and K. K. Swartz (Springer, New York, 1982), p. 61.
[2]K. Knorr and A. Loidl, Phys. Rev. B **31**, 5387 (1985).
[3]H. U. Beyeler, Phys. Rev. B **11**, 3078 (1975).
[4]J. J. De Yoreo, W. Knaak, M. Meissner, and R. O. Pohl, Phys. Rev. B **34**, 8828 (1986).
[5]J. N. Dobbs, M. C. Foote, and A. C. Anderson, Phys. Rev. B **33**, 4178 (1986).
[6]W. D. Seward and V. Narayanamurti, Phys. Rev. **148**, 463 (1966).
[7]A. L. Varma, J. Phys. C **13**, 2009 (1980).
[8]J. M. Rowe, J. J. Rish, D. G. Hinks, and S. Susman, Phys. Rev. Lett. **33**, 412 (1978).
[9]S. K. Satija and C. H. Wang, Solid State Commun. **28**, 617 (1978).
[10]U. T. Höchli, K. Knorr, and A. Loidl, Adv. Phys. **39**, 405 (1990).
[11]J. P. Sethna and K. S. Chow, Phase Trans. **5**, 317 (1985).
[12]M. Meissner, W. Knaak, J. P. Sethna, K. S. Chow, J. J. De Yoreo, and R. O. Pohl, Phys. Rev. B **32**, 6091 (1985).
[13]J. F. Berret, P. Doussineau, A. Levelut, M. Meissner, and W. Schön, Phys. Rev. Lett. **55**, 2013 (1985).
[14]M. C. Foote and B. Golding, J. Phys. Condens. Matter **1**, 7751 (1989).
[15]D. Moy, J. N. Dobbs, and A. C. Anderson, Phys. Rev. B **29**, 2160 (1984).
[16]W. A. Phillips, J. Low Temp. Phys. **7**, 351 (1972).
[17]P. W. Anderson, B. I. Halperin, and C. M. Varma, Philos. Mag. **25**, 1 (1972).
[18]For a review, see B. Golding and J. E. Graebner, in *Amorphous Solids,* edited by W. A. Phillips, Topics in Current Physics Vol. 24 (Springer-Verlag, 1984), p. 107.
[19]M. C. Foote and B. Golding, Phys. Rev. B **43**, 9206 (1991).
[20]G. Baier, M. v. Schickfus, and C. Enss, Europhys. Lett. **8**, 487 (1989).
[21]M. W. Klein, Phys. Rev. B **29**, 5825 (1984); **40**, 1918 (1989).
[22]A. Yariv, *Quantum Electronics* (Wiley, New York, 1988), p. 351.
[23]R. P. Feynman, F. L. Vernon, Jr., and R. W. Hellwarth, J. Appl. Phys. **28**, 49 (1957).
[24]J. L. Black and B. I. Halperin, Phys. Rev. B **16**, 2879 (1977).
[25]B. D. Laikhtman, Phys. Rev. B **31**, 490 (1985).
[26]V. L. Gurevich, M. I. Muradov, and D. A. Parshin, Zh. Eksp. Teor. Fiz. **97**, 1644 (1990) [Sov. Phys. JETP **70**, 928 (1990)].
[27]F. Bloch, Phys. Rev. **70**, 460 (1946).
[28]J. Jäckle, Z. Phys. **257**, 212 (1972).
[29]G. Baier, C. Enss, and M. v. Schickfus, Phys. Rev. B **40**, 9868 (1989).
[30]C. Enss, D. Arndt, and M. v. Schickfus, in *Phonon Scattering in Condensed Matter VII,* edited by M. Meissner and R. O. Pohl (Springer, New York, 1992), p. 321.
[31]T. Janssen, Phys. Kondens. Materie **15**, 205 (1972).
[32]C. P. Slichter, *Principles of Magnetic Resonance,* 2nd ed., Springer Series in Solid State Sciences Vol. 1 (Springer-Verlag, New York, 1980).
[33]B. Golding and J. E. Graebner, Phys. Rev. B **19**, 964 (1979).
[34]P. Hu and L. R. Walker, Solid State Commun. **24**, 813 (1977).
[35]N. C. Wong, S. S. Kono, and R. G. Brewer, Phys. Rev. A **21**, 260 (1980).
[36]G. Baier and M. v. Schickfus, Phys. Rev. B **38**, 9952 (1988).
[37]The samples, seed-pulled from the melt under a protective atmosphere, were grown by S. Haussühl at the University of Cologne. Starting material was KBr "Suprapur" from Merck with the major impurities stated as iodine (<500 ppm) and chlorine (<200 ppm). CN^- concentrations were verified by infrared spectroscopy.
[38]It should be noted that, although Eq. (22) is also valid for glasses, ω_d cannot be neglected in this case because of the broad distribution of tunnel splitting in amorphous materials.
[39]C. Enss, H. Schwoerer, D. Arndt, M. v. Schickfus, and G.

Weiss, Europhys. Lett. **26**, 289 (1994).
[40]M. W. Klein, Phys. Rev. Lett. **65**, 3017 (1990).
[41]H. S. Sack and M. C. Moriarty, Solid State Commun. **3**, 93 (1965).
[42]L. Bernard, L. Piche, G. Schumacher, and J. Joffrin, J. Low Temp. Phys. **35**, 411 (1979).
[43]E. L. Hahn, Phys. Rev. **80**, 580 (1950).
[44]B. Golding, M.v. Schickfus, S. Hunklinger, and K. Dransfeld, Phys. Rev. Lett. **43**, 1817 (1979).